

Chromosome missegregation rate predicts whether aneuploidy will promote or suppress tumors

Alain D. Silk^{a,b,c,d,1}, Lauren M. Zasadil^{e,f,1}, Andrew J. Holland^{a,b,2}, Benjamin Vitre^{a,b}, Don W. Cleveland^{a,b,3}, and Beth A. Weaver^{e,g,3}

^aLudwig Institute for Cancer Research and ^bDepartment of Cellular and Molecular Medicine, University of California at San Diego, La Jolla, CA 92093; ^cDepartment of Dermatology and ^dKnight Cancer Institute, Oregon Health and Science University, Portland, OR 97239; ^eDepartment of Cell and Regenerative Biology, ^fMolecular Pharmacology Training Program, and ^gCarbone Cancer Center, University of Wisconsin, Madison, WI 53705

Contributed by Don W. Cleveland, September 13, 2013 (sent for review July 2, 2013)

Aneuploidy, a chromosome content other than a multiple of the haploid number, is a common feature of cancer cells. Whole chromosomal aneuploidy accompanying ongoing chromosomal instability in mice resulting from reduced levels of the centromere-linked motor protein CENP-E has been reported to increase the incidence of spleen and lung tumors, but to suppress tumors in three other contexts. Exacerbating chromosome missegregation in CENP-E^{+/-} mice by reducing levels of another mitotic checkpoint component, Mad2, is now shown to result in elevated cell death and decreased tumor formation compared with reduction of either protein alone. Furthermore, we determine that the additional contexts in which increased whole-chromosome missegregation resulting from reduced CENP-E suppresses tumor formation have a preexisting, elevated basal level of chromosome missegregation that is exacerbated by reduction of CENP-E. Tumors arising from primary causes that do not generate chromosomal instability, including loss of the INK4a tumor suppressor and microsatellite instability from reduction of the DNA mismatch repair protein MLH1, are unaffected by CENP-E-dependent chromosome missegregation. These findings support a model in which low rates of chromosome missegregation can promote tumorigenesis, whereas missegregation of high numbers of chromosomes leads to cell death and tumor suppression.

Mad2 | ARF | spindle assembly checkpoint | CIN

Aneuploidy resulting from errors in mitosis was initially recognized more than 100 y ago as a common feature of tumor cells (1). Boveri proposed in 1902 (2) and 1914 (3) that the primordial cells of tumors are aneuploid. However, whether aneuploidy is a cause or effect of tumorigenesis has remained controversial. Indeed, Boveri's attempts at generating aneuploidy in sea urchin embryos through multipolar mitoses most often resulted in cell death (3). More recently, the finding that high rates of chromosome missegregation lead to cell death has been extended to cancer cells, which undergo cell-autonomous lethality in response to massive chromosome missegregation caused by multipolar divisions or complete inactivation of the mitotic checkpoint (4–6).

We recently tested the hypothesis that aneuploidy drives tumor initiation and/or progression by examining tumor development in mice with reduced levels of CENP-E, a large (~312 kDa in human) centromere-bound motor protein responsible for powering congression of initially misaligned chromosomes (7, 8). CENP-E accumulates in late G2, functions during mitosis, and is degraded at the end of mitosis as quantitatively as cyclin B (9). During mitosis, CENP-E localizes to kinetochores, where it is one of a number of proteins that serve as linkers between chromosomes and the microtubules of the mitotic spindle (10–12). Reduction of CENP-E results in the chronic misalignment of one or a few chromosomes near the spindle poles, on which at least one kinetochore per chromatid pair remains unbound to microtubules (10, 11). Heterozygous reduction of CENP-E leads to the missegregation of one or a few chromosomes per

division without causing DNA damage or chromosomal rearrangements (13).

CENP-E also functions in the mitotic checkpoint (also known as the spindle assembly checkpoint), the major cell cycle control mechanism acting during mitosis to prevent chromosome missegregation and aneuploidy (14, 15). Normally, even a single unattached kinetochore is sufficient to sustain mitotic checkpoint activation (16, 17). However, the mitotic checkpoint is weakened after reduction of CENP-E, and CENP-E^{+/-} cells enter anaphase in the presence of one or a few misaligned chromosomes, thereby producing aneuploid progeny as the result of a low rate of chromosomal instability (CIN) (10–13, 15). CENP-E has no known function(s) outside of mitosis.

CENP-E^{+/-} animals are overtly normal throughout the majority of their lifespan. Aged CENP-E^{+/-} animals develop spontaneous spleen and lung tumors more frequently than wild-type littermates. Unexpectedly, however, reduction of CENP-E prolongs tumor latency after homozygous deletion of the ARF tumor suppressor (also known as p19, p19ARF, or p14ARF in human). Additionally, CENP-E^{+/-} animals develop fewer and smaller spontaneous liver tumors and fewer tumors after treatment with the carcinogen 7,12-Dimethylbenz(a)anthracene (DMBA) (13). These findings are consistent with aneuploidy resulting from low CIN producing genetic context-specific effects on tumor initiation and progression, although the mechanism is not established.

Significance

Aneuploidy, an abnormal chromosome content that commonly occurs because of errors in chromosome segregation, can promote or suppress tumor formation. What determines how aneuploidy influences tumorigenesis has remained unclear. Here we show that the rate of chromosome missegregation, rather than the level of accumulated aneuploidy, determines the effect on tumors. Increasing the rate of chromosome missegregation beyond a certain threshold suppresses tumors by causing cell death. Increasing errors of chromosome segregation did not affect tumor formation caused by genetic mutations that do not themselves alter chromosome inheritance. These results suggest that accelerating chromosome missegregation in chromosomally unstable tumors may be a useful strategy therapeutically.

Author contributions: A.D.S., L.M.Z., D.W.C., and B.A.W. designed research; A.D.S., L.M.Z., A.J.H., B.V., and B.A.W. performed research; A.D.S., L.M.Z., A.J.H., B.V., and B.A.W. analyzed data; and D.W.C. and B.A.W. wrote the paper.

The authors declare no conflict of interest.

¹A.D.S. and L.M.Z. contributed equally to this work.

²Present address: Department of Molecular Biology and Genetics, The Johns Hopkins University School of Medicine, Baltimore, MD 21205.

³To whom correspondence may be addressed. E-mail: dcleveland@ucsd.edu or baweaver@wisc.edu.

This article contains supporting information online at www.pnas.org/lookup/suppl/doi:10.1073/pnas.1317042110/-DCSupplemental.

Genomic instability has been proposed as an enabling characteristic for tumor formation. Two types of genomic instability frequently occur in cancer cells: CIN and microsatellite instability (MIN), in which reduced activity of mismatch repair (MMR) genes leads to an increase in DNA mutation. It is well established that the low rate of DNA mutation caused by reduction of MMR proteins promotes tumorigenesis, but a high rate of DNA mutation, caused by radiation or chemotherapy drugs such as cisplatin, leads to rapid cell death (18–20). By specifically generating aneuploidy in the absence of other genomic defects, we show here that CIN behaves similarly: Low CIN can promote tumors, but high CIN leads to cell death and tumor suppression. Genetic backgrounds and tissue types in which the reduction of CENP-E leads to tumor suppression have a preexisting, elevated rate of CIN with one or a few chromosomes missegregated per division. Reduction of CENP-E in these

contexts produces a significantly elevated rate of chromosomal missegregation, resulting in high CIN, cell death, and tumor suppression.

Results

ARF Loss Causes a Low Rate of Chromosome Missegregation That Is Exacerbated by Reduction of CENP-E. In an attempt to understand the differing effects of CENP-E heterozygosity on tumors arising from divergent initiating events, we tested whether contexts in which reduction of CENP-E led to tumor suppression exhibited CIN. Recognizing that CENP-E heterozygosity suppresses tumors in ARF^{-/-} mice, aneuploidy was determined in low-passage primary murine embryonic fibroblasts (MEFs) obtained from embryonic day 14.5 ARF^{-/-} embryos. Although no role for ARF in maintenance of chromosomal stability has been proposed previously, loss of ARF induced aneuploidy in primary MEFs and

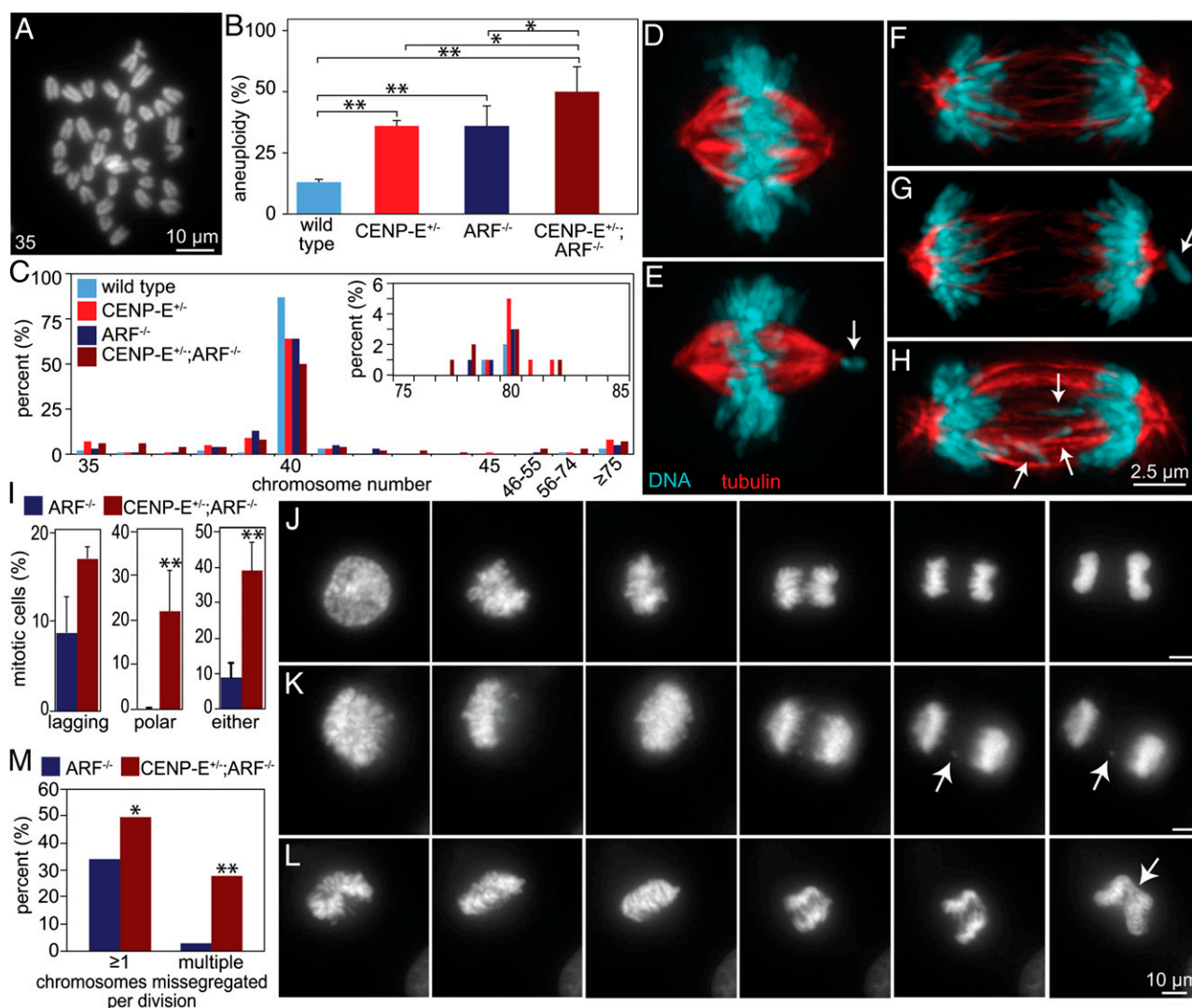


Fig. 1. ARF loss results in low CIN that is exacerbated by reduction of CENP-E. (A) Representative mitotic chromosome spread from a primary MEF. The number "35" indicates the number of chromosomes in the example shown. (B) Aneuploidy levels in primary cells of the indicated genotypes at passage 3 ($n = 100$ per genotype; $*P < 0.05$; $**P < 0.001$). (C) Chromosome numbers in primary MEFs ($n = 100$) of the genotypes shown in B. Inset shows the percentage of cells containing 75–85 chromosomes. (D–H) Immunofluorescence images of mitotic figures from CENP-E^{+/-}; ARF^{-/-} MEFs. (D) Normal metaphase. (E) Pseudo-metaphase; arrow indicates a polar chromosome. (F) Normal anaphase. (G) Abnormal anaphase; arrow indicates a polar chromosome. (H) Abnormal anaphase; arrows indicate lagging chromosomes. (I) Quantitation of aberrant mitotic figures ($n > 500$ cells from two independent experiments; $**P < 0.001$). (J–L) Stills from [Movies S1–S3](#) of cells with fluorescent chromosomes in mitosis, including normal division (J), a CENP-E^{+/-}; ARF^{-/-} cell with one lagging chromosome (arrows) (K), and missegregation of many chromosomes (arrow) in a CENP-E^{+/-}; ARF^{-/-} cell (L). (Scale bars, 10 μ m.) (M) Quantitation of cells that missegregate ≥ 1 chromosome (Left) or ≥ 2 chromosomes (Right). $*P < 0.05$; $**P < 0.001$.

did so to a level equivalent to heterozygous loss of CENP-E (Fig. 1 *A* and *B*). Aneuploidy was increased even further, to 50%, in CENP-E^{+/-};ARF^{-/-} cells (Fig. 1*B*). Like CENP-E^{+/-} cells, ARF^{-/-} aneuploid cells were predominantly near-diploid, with a minor population of tetraploid and near-tetraploid cells (Fig. 1*C*).

Consistent with their aneuploid status, ARF^{-/-} and CENP-E^{+/-};ARF^{-/-} cells displayed abnormal mitotic figures indicative of chromosome missegregation. These included chromosomes that remained associated with one of the spindle poles (polar chromosomes), despite congression of the others, to produce pseudo-metaphase (Fig. 1*D* and *E*). A portion of these polar chromosomes continued well into anaphase (Fig. 1*F* and *G*). Additional chromosome segregation errors included chromosomes that lagged behind the segregating masses of DNA during anaphase and telophase (lagging chromosomes; Fig. 1*H*). Although lagging chromosomes were the most common abnormality observed in ARF^{-/-} cells, CENP-E^{+/-};ARF^{-/-} MEFs exhibited both polar and lagging chromosomes (Fig. 1*I*). Taken together, CENP-E^{+/-};ARF^{-/-} cells exhibited a significantly higher percentage of abnormal mitotic figures consistent with chromosome missegregation than ARF^{-/-} cells with normal CENP-E content (Fig. 1*I*).

Missegregation was also followed by live-cell analysis in MEFs with fluorescent chromosomes produced by stable expression of histone H2B-RFP. Although many cells underwent a normal mitosis in which all chromosomes aligned at the spindle equator before segregating equally to produce two genetically identical daughter cells (Fig. 1*J* and *Movie S1*), 34% (11 of 32) of ARF^{-/-} MEFs missegregated one or more chromosomes (Fig. 1*K* and *M* and *Movie S2*). This rate increased to 50% (17 of 34 cells) after reduction of CENP-E (Fig. 1*L* and *M* and *Movie S3*). Although most ARF^{-/-} cells (10 of 11 cells; 91%) missegregated only a single chromosome, the majority of CENP-E^{+/-};ARF^{-/-} cells (10 of 17; 58%) missegregated multiple chromosomes (Fig. 1*M*). These data are consistent with the findings in fixed cells and demonstrate that ARF^{-/-} cells have a preexisting, basal rate of CIN that is increased by reduction of CENP-E.

Liver Cells Have a Low Rate of Chromosome Missegregation That Is Increased by Reduction of CENP-E. Liver tumor size and number are reduced in CENP-E heterozygous animals relative to wild-type littermates. Liver cells are known to exhibit aneuploidy, polyploidy, and CIN (11, 21). To determine whether reduction of CENP-E caused an increase in the rate of CIN in the liver, mitoses were examined in 2- to 3-mo-old animals injected with carbon tetrachloride to induce hepatocyte proliferation in response to liver damage (Fig. 2*A*). Anaphase and telophase figures in H&E-stained liver sections were inspected for evidence of chromosome missegregation. Although normal anaphase figures were present (Fig. 2*B*), many wild-type cells exhibited lagging chromosomes (Fig. 2*C*, arrow), consistent with published reports of aneuploidy in normal liver (21, 22). Polar chromosomes (Fig. 2*D*, arrows) were common in cells with reduced levels of CENP-E resulting from the inactivation of a conditional allele (with Adeno-Cre) (11). On average, wild-type hepatocytes missegregated a single chromosome per division (range, 0–5) (Fig. 2*E* and *F*). Cells with reduced levels of CENP-E, however, missegregated four chromosomes per division on average (range, 0–10) (Fig. 2*E* and *F*). Thus, liver cells exhibit low CIN that is exacerbated by reduction of CENP-E.

DMBA Treatment Causes Low CIN That Is Exacerbated by Reduction in CENP-E. The third context in which tumor suppression has been observed when CENP-E is reduced is treatment with the carcinogen DMBA (13). DMBA is a well-characterized mutagen. Consistent with this evidence, DMBA treatment caused a large increase in phosphorylated histone H2AX reactivity, a marker of dsDNA breaks (Fig. 3*A*). DMBA also caused chromatid gaps,

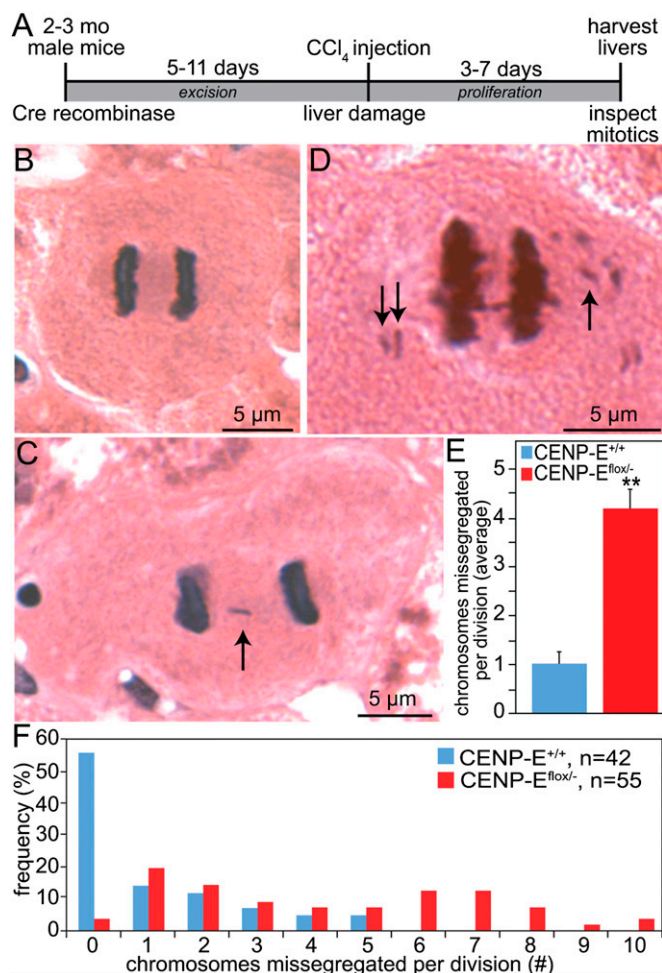


Fig. 2. Liver cells exhibit low CIN that is increased by reduction of CENP-E. (*A*) Schematic of experiment to initiate proliferation in murine hepatocytes with normal and reduced levels of CENP-E by introducing an adenovirus encoding Cre recombinase into 2- to 3-mo-old mice with wild-type CENP-E (^{+/+}) or one floxed and one null allele of CENP-E (^{flox/-}) (11). (*B–D*) H&E-stained tissue sections of mitotic hepatocytes in normal anaphase (*B*), anaphase with lagging chromosome (arrow) (*C*), and anaphase with polar chromosomes (arrows) (*D*). (*E* and *F*) Average number (\pm SEM) (*E*) and range (*F*) of chromosomes not contained within the segregating masses of DNA obtained by analysis of wild-type ($n = 42$) and CENP-E^{flox/-} ($n = 55$) cells. *****P* < 0.001**.

chromosome fragments, and multiradial chromosomes, as observed in metaphase spreads (Fig. 3*B*).

When MEFs were examined for abnormal mitoses after exposure to DMBA, the percentage of cells in mitosis was found to drop noticeably in both wild-type and CENP-E^{+/-} cells (Fig. 3*C*), consistent with an intact DNA damage response in wild-type and CENP-E^{+/-} MEFs. However, examination of the cells that did enter mitosis revealed that DMBA-treated cells with normal CENP-E content had an increased level of lagging chromosomes in anaphase and telophase (Fig. 3*D*, *Left*). CENP-E^{+/-} cells had increased levels of polar chromosomes in the presence and absence of DMBA (Fig. 3*D*, *Center*). DMBA treatment caused an increase in lagging chromosomes in CENP-E^{+/-} cells (Fig. 3*D*, *Left*). Together, CENP-E^{+/-} cells treated with DMBA had a significantly higher proportion of abnormal mitotic figures, consistent with an elevated rate of chromosome missegregation relative to wild-type cells treated with DMBA (Fig. 3*D*, *Right*). Thus, DMBA causes a low rate of CIN that is exacerbated by reduction of CENP-E.

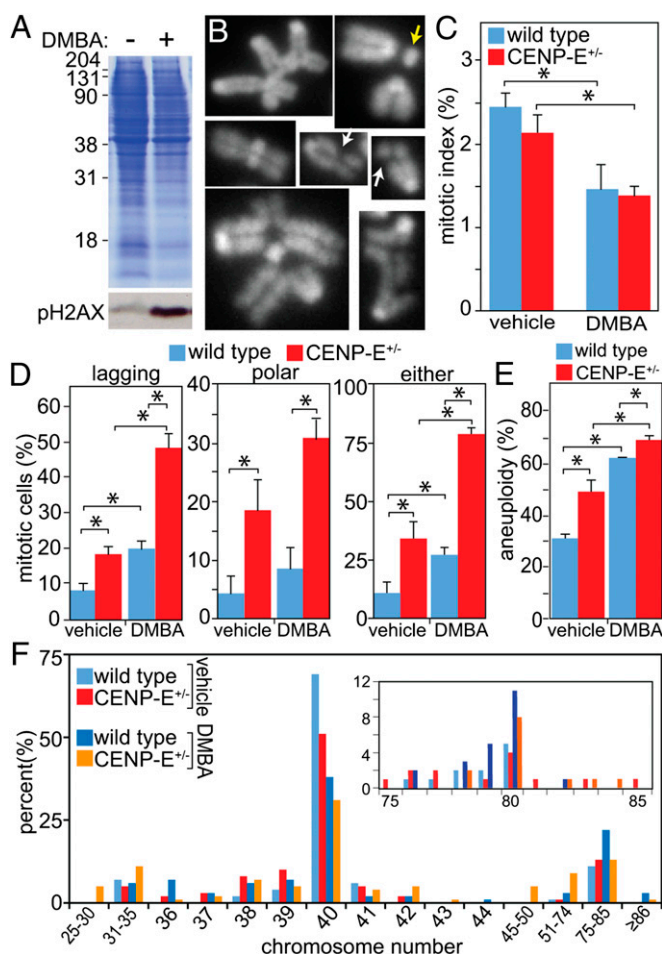


Fig. 3. DMBA treatment causes a low rate of CIN that is exacerbated by heterozygous loss of CENP-E. (A) Assay for DNA damage by gel electrophoresis of extracts from cells treated or not with DMBA and immunoblotted for phosphorylated histone H2AX. Coomassie, loading control. (B) Images of chromosomes isolated from mitotic cells 72 h after treatment with DMBA which display defects consistent with DNA damage, including chromatid gaps (white arrows), fragments (yellow arrow) and multiradial chromosomes (Top Left). (C) Mitotic indices of primary cells treated with vehicle or DMBA for 24 h ($n > 2,000$ cells from three independent experiments; $*P < 0.05$). (D) Quantitation of lagging chromosomes (Left), polar chromosomes (Center), or either aberrant positioning after 24 h treatment with vehicle or DMBA (Right) ($n > 150$ cells from three independent experiments; $*P < 0.05$). (E) Aneuploidy developed by cells at passage 3 with normal or lowered CENP-E after incubation in 50 $\mu\text{g/mL}$ DMBA for 72 h ($n = 100$; $*P < 0.05$). (F) Histogram of chromosome numbers per cell after 72 h of treatment with 50 $\mu\text{g/mL}$ DMBA. Inset shows percentage of cells with tetraploid and near-tetraploid chromosome numbers between 75 and 85.

Examination of primary MEFs revealed that DMBA treatment is sufficient to increase aneuploidy in wild-type cells, as scored in metaphase spreads (Fig. 3E, blue bars), consistent with the observed increase in lagging chromosomes. Treatment of CENP-E^{+/-} MEFs with DMBA further increased the incidence of aneuploidy (Fig. 3E, red bars). Examination of chromosome numbers revealed that, unlike CENP-E reduction or ARF loss, DMBA treatment resulted in low percentages of near-triploid cells as well as polyploid cells with chromosome numbers of 140–160 (Fig. 3F). Interestingly, as for ARF loss, the increase in aneuploidy resulting from the reduction of CENP-E combined with DMBA treatment was not fully additive (Fig. 3E), a result that is consistent with some aneuploid cells being eliminated from the population.

Reduction of CENP-E Causes High CIN and Tumor Suppression in Mad2^{+/-} Animals. CENP-E heterozygosity suppressed tumorigenesis in the ARF^{-/-} background, in mouse liver, and after DMBA treatment, three contexts in which CENP-E loss also elevated preexisting basal rates of CIN. These results suggested that reducing CENP-E in a context that already exhibited low CIN because of the depletion of another component of the mitotic checkpoint would result in high CIN and tumor suppression. To test this hypothesis, CENP-E^{+/-} mice were bred with animals heterozygous for mitotic arrest deficient 2 (Mad2), the initiating component of the mitotic checkpoint whose conformational change is produced by unattached kinetochores as the first of two catalytic steps that inhibit activation of the anaphase-promoting complex (23), thereby blocking advance to anaphase. Mad2^{+/-} cells develop aneuploidy, accompanied by low CIN, similar to CENP-E^{+/-} cells (24, 25). Like CENP-E^{+/-} animals, aged Mad2^{+/-} mice develop lung adenomas (25).

CENP-E^{+/-};Mad2^{+/-} double heterozygous animals were generated by CENP-E^{+/-} × Mad2^{+/-} crosses. CENP-E^{+/-};Mad2^{+/-} animals were born at expected frequencies ($24 \pm 3\%$; $n = 11$) and remained viable. Like CENP-E^{+/-} animals, Mad2^{+/-} and CENP-E^{+/-};Mad2^{+/-} double heterozygous animals developed normal body (Fig. S1 A and B) and organ weights (Fig. S1 C–E) and were overtly normal throughout their lifespans.

Examination of mitoses confirmed that CENP-E^{+/-};Mad2^{+/-} double heterozygous cells exhibit a higher rate of CIN than CENP-E^{+/-} or Mad2^{+/-} MEFs. CENP-E^{+/-} and CENP-E^{+/-};Mad2^{+/-} MEFs contained elevated levels of polar chromosomes, whereas Mad2^{+/-} and CENP-E^{+/-};Mad2^{+/-} double heterozygous cells had lagging chromosomes in anaphase and telophase (Fig. 4A). Together, cells heterozygous for both Mad2 and CENP-E had a significantly higher proportion of abnormal mitotic figures than cells with reduced levels of CENP-E or Mad2 alone, indicative of an elevated rate of chromosome mis-segregation (Fig. 4A). Therefore, Mad2^{+/-} cells exhibit low CIN that is exacerbated by reduction of CENP-E.

To determine how high CIN in CENP-E^{+/-};Mad2^{+/-} double heterozygous cells affected tumorigenesis, 19- to 21-mo-old wild-type, CENP-E^{+/-}, Mad2^{+/-}, and CENP-E^{+/-};Mad2^{+/-} animals were euthanized and examined for tumors. In addition to the lung adenomas reported in a previous study (25), we also observed splenic lymphomas in the Mad2^{+/-} mice in our cohort. CENP-E^{+/-} mice developed splenic lymphomas and lung adenomas to a similar extent as Mad2^{+/-} animals (Fig. 4 B and C). Lymphomas displayed replacement of normal splenic follicles (Fig. 4B, Center) with a proliferation of neoplastic cells (Fig. 4B, Right). Adenomas exhibited a dense, glandular appearance (Fig. 4C, Right) compared with the lacelike structure of normal lung (Fig. 4C, Center). However, CENP-E^{+/-};Mad2^{+/-} double heterozygous animals developed no splenic tumors and had a two- to threefold decrease in adenomas of the lung (Fig. 4C, Left). Therefore, reduction in CENP-E and the accompanying increase in the rate of CIN in Mad2^{+/-} animals led to tumor suppression.

Reduction of CENP-E Does Not Suppress Tumors Caused by Loss of INK4a, a Tumor Suppressor That Does Not Prevent CIN. The preceding data support the hypothesis that CENP-E reduction suppresses tumors in contexts with an elevated basal rate of CIN. These results suggest that reduction of CENP-E does not extend tumor-free survival in animals that develop tumors in the absence of CIN. To test this possibility more directly, we mated CENP-E^{+/-} animals with animals lacking the INK4a tumor suppressor, which develop tumors because of deregulated cell-cycle control at the G1→S transition. INK4a inhibits the cyclin D-dependent kinases CDK4 and CDK6. Together with cyclin E/CDK2, cyclin D/CDK4 and cyclin D/CDK6 control entry into S phase by hyperphosphorylating the Rb tumor suppressor (26).

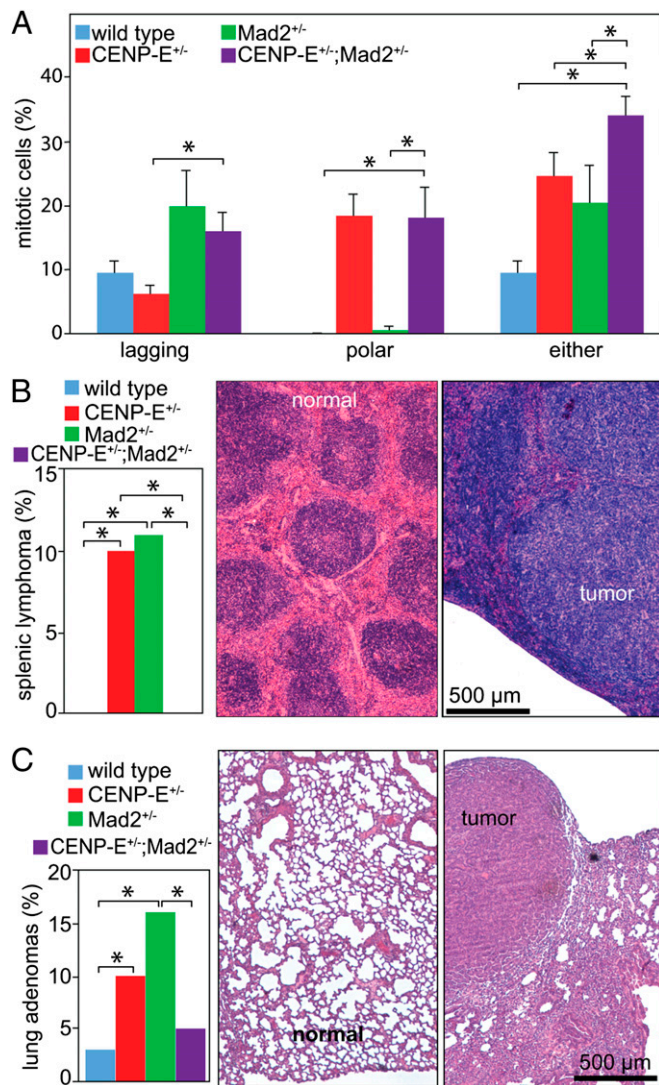


Fig. 4. Reduction of CENP-E in $Mad2^{+/-}$ cells and mice leads to high CIN and tumor suppression. (A) Quantitation of aberrant mitotic figures in primary MEFs of the indicated genotypes (mean \pm SEM, $n = 4$). (B) (Left) Frequency of splenic lymphomas in CENP-E^{+/-};Mad2^{+/-} doubly heterozygous or CENP-E^{+/-} or Mad2^{+/-} singly heterozygous mice. H&E-stained tissue sections of normal spleen (Center) and splenic lymphoma (Right) ($*P < 0.05$). (C) (Left) Frequency of lung adenomas is diminished in CENP-E^{+/-};Mad2^{+/-} mice with the highest level of CIN; H&E-stained tissue sections of normal lung (Center) and lung adenoma (Right) ($n = 30$ wild-type, 30 CENP-E^{+/-}, 19 Mad^{+/-}, and 21 CENP-E^{+/-};Mad2^{+/-}). $*P < 0.05$ in all panels.

Loss of Rb has been reported to drive centrosome amplification, tetraploidy, and aneuploidy (27, 28). However, loss of INK4a does not result in centrosome amplification, tetraploidy, or aneuploidy in human cells (29), and INK4a^{-/-} MEFs do not exhibit significantly elevated levels of abnormal mitotic figures or develop aneuploidy or tetraploidy (Fig. S2 A and B). As expected, addition of CENP-E heterozygosity increased the rate of chromosome missegregation in INK4a^{-/-} cells (Fig. S2 A and B).

Any of three outcomes were possible. If reduction of CENP-E causes tumor suppression only by enhancing a preexisting basal rate of CIN, as opposed to another mechanism, reduction of CENP-E should not cause tumor suppression in INK4a^{-/-} animals. Conversely, if increased aneuploidy caused by the reduction of CENP-E suppresses tumors irrespective of the rate of CIN, an increased tumor latency in CENP-E^{+/-};INK4a^{-/-} ani-

mals would be expected. Last, if increasing CIN uniformly promotes tumors, reduction of CENP-E would be predicted to reduce tumor latency in INK4a^{-/-} mice, as has been seen after reduction of BubR1 (30). To test among these possibilities, we bred CENP-E^{+/-} animals with INK4a^{-/-} mice. Subsequent crosses produced CENP-E^{+/-};INK4a^{-/-} animals and INK4a^{-/-} littermates. Reduction of CENP-E had no significant effect on either tumor-free or overall survival in INK4a^{-/-} animals (Fig. S2 C and D), findings supporting the hypothesis that reduction of CENP-E causes tumor suppression only in contexts with a preexisting, elevated rate of genomic instability.

Low CIN Caused by Reduction of CENP-E Does Not Cooperate with MIN. MIN and CIN rarely occur in the same tumors (31), perhaps because a combination of the two produces a higher level of genomic instability than can be tolerated by cells. To test if CENP-E-mediated CIN affected tumorigenesis from loss of the MLH1 tumor suppressor, CENP-E^{+/-} animals were crossed with MLH1^{+/-} animals. *MLH1* encodes an MMR protein and, when mutated in the germ line, causes hereditary nonpolyposis colorectal cancer (32). Reduction of MLH1 in mice results in increased tumorigenesis, with no increase in chromosome missegregation or aneuploidy (Fig. S3 A–C and ref. 18). CENP-E heterozygosity increased chromosome missegregation and aneuploidy in MLH1^{-/-} MEFs, as expected (Fig. S3 A–C). If low CIN caused tumor suppression in the presence of MIN, reduction of CENP-E should extend tumor latency in MLH1^{+/-} animals. However, neither tumor-free nor overall survival of MLH1^{+/-} and CENP-E^{+/-};MLH1^{+/-} littermates differed significantly (Fig. S3 D and E), demonstrating that increasing whole chromosomal aneuploidy in the presence of MIN from errors in DNA mismatch repair does not affect MIN-mediated tumors.

High CIN Causes Increased Cell Death. Although aneuploidy levels were elevated in CENP-E^{+/-};ARF^{-/-} MEFs (50% aneuploidy) compared with cells with reduced levels of either ARF or CENP-E alone (36% aneuploidy in each case), the increase in aneuploidy was less than the sum of the individual aneuploidies (Fig. 1B). Similarly, DMBA-treated CENP-E^{+/-} MEFs showed an increased (and very high) level of aneuploidy (69% of cells aneuploid), but one that still is lower than the 100% that would reflect adding the frequency of aneuploid cells resulting from DMBA treatment and reduction of CENP-E. Additionally, despite an increased rate of CIN in CENP-E^{+/-};Mad2^{+/-} MEFs (Fig. 4A), CENP-E^{+/-};Mad2^{+/-} cells did not show increased aneuploidy compared with cells with reduced levels of CENP-E or Mad2 alone. This finding was true in MEFs in vitro (Fig. S1 F) as well as in colonic crypt cells in vivo (Fig. S1 G and H). These data suggest that some aneuploid cells are being eliminated, consistent with a tumor-suppressive effect of elevating the rate of chromosome missegregation in the context of preexisting CIN.

It has been shown previously that high CIN, caused either by multipolar divisions or by complete inactivation of the mitotic checkpoint, leads to rapid cell death, presumably because of the loss of both copies of one or more essential chromosomes (4–6). We tested whether high CIN caused by the combination of two insults, each of which produced a low rate of CIN, also resulted in cell death. Indeed, reduction of CENP-E in ARF^{-/-} cells led to increased cell death, as scored by DNA morphology and/or caspase-3 activity (Fig. 5 A and B). Similarly, CENP-E^{+/-} cells were more sensitive than wild-type cells to DMBA treatment (Fig. 5 C–E). Fewer CENP-E^{+/-} than wild-type cells survived 72 h of treatment with 50 μ g/mL DMBA (Fig. 5 C and D), and CENP-E^{+/-} MEFs had higher levels of cell death than wild-type cells in response to DMBA (Fig. 5 E), which causes both DNA mutation and increased aneuploidy (Fig. 3). CENP-E^{+/-} cells were not more sensitive to doxorubicin, which causes DNA damage without widespread aneuploidy (Fig. 5 F). Reduction of

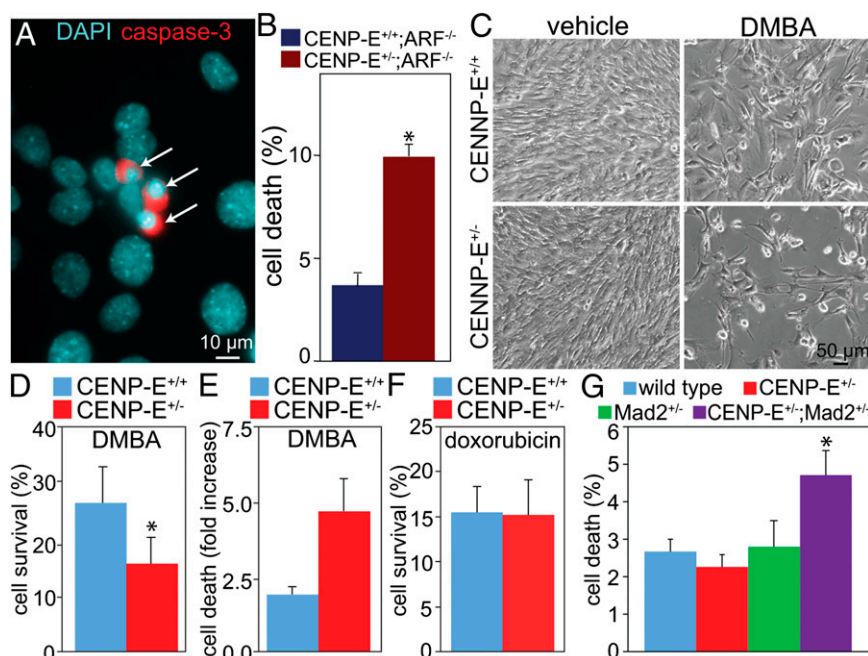


Fig. 5. High CIN causes increased cell death. (A and B) Cell death rates in $ARF^{-/-}$ cells with or without CENP-E, as scored by DNA morphology and/or activation of caspase-3. (A) DNA is shown in blue; activated caspase-3 is shown in red; arrows indicate dead cells. (B) Cell death in asynchronously cycling primary MEFs ($n \geq 200$ cells from each of five or more independent experiments; $*P < 0.05$). (C–E) Sensitivity of CENP-E $^{+/-}$ cells to DMBA. (C) Phase-contrast images of cells treated with DMBA or vehicle (acetone) alone for 72 h. (D) Cell survival, as scored by counting with a hemacytometer, after 72 h of treatment with DMBA or vehicle and normalized to survival without DMBA treatment ($n = 4$; $*P < 0.05$). (E) Cell death caused by DMBA treatment, reported as the increase in percentage of cell death in DMBA-treated versus control cells ($n = 2$). (F) Measurement of sensitivity of CENP-E $^{+/-}$ cells versus wild-type cells to DNA damage caused by doxorubicin. Cell survival, relative to untreated cells, is shown after 72 h treatment with 0.3 $\mu\text{g}/\text{mL}$ doxorubicin ($n = 3$). (G) Cell death in asynchronously cycling primary MEFs of the indicated genotypes ($n > 500$ cells from each of four independent experiments; $*P < 0.05$).

CENP-E in $Mad2^{+/-}$ cells also resulted in increased cell death, compared with reduction of CENP-E or $Mad2$ alone (Fig. 5G). Thus, three genetic contexts in which reduction of CENP-E led to tumor suppression all individually showed CIN and an increase in cell death when combined with additional whole chromosomal segregation errors that accompany reduction in CENP-E.

Discussion

A cause-and-effect relationship between aneuploidy and cancer has been difficult to define (13). To our earlier evidence that a modestly elevated rate of whole-chromosome missegregation resulting from a reduction in CENP-E results in an increased rate of tumor induction, we have shown here that even higher rates of chromosome missegregation enhance cell death and suppress tumorigenesis. This result establishes whole-chromosome aneuploidy as one of the factors that can both promote and inhibit tumor initiation and/or progression, depending on the context (33), like the well-accepted examples of *Ras* (34) and *Myc* (35, 36). In the case of aneuploidy, multiple lines of evidence now support the conclusion that low rates of chromosome missegregation can promote tumorigenesis, whereas higher rates of chromosome missegregation lead to cell death and tumor suppression.

Reduction of CENP-E causes an increase both in the percentage of abnormal mitoses and in the number of chromosomes missegregated per division. Despite the increase in chromosome missegregation, not every division is abnormal. High CIN that is sufficient to cause cell death therefore could result from missegregation of large numbers of chromosomes in a single division and/or from an increase in the frequency of abnormal divisions. Mis-segregation of a small number of chromosomes per division in a substantial portion of divisions (approximately one-quarter; Fig. 4A) is not sufficient to increase the level of cell death (Fig.

5G), and populations of CENP-E $^{+/-}$ cells do not exhibit a growth defect (13). Rather, cell death increases in populations that missegregate higher numbers of chromosomes in a single division. This finding is consistent with earlier reports that $BubR1^{+/-}$ MEFs, which missegregate small numbers of chromosomes, do not have a growth defect (37), but $\sim 90\%$ depletion of *BubR1* leads to missegregation of large numbers of chromosomes per division and rapid cell death (38). It also is consistent with a report that populations containing cells that missegregated more than five chromosomes per division had decreased colony-forming ability compared with those that missegregated one to five chromosomes in a single division (38). Taken together, these data suggest that CIN sufficiently high to cause cell death arises from an increase in the number of chromosomes missegregated per division.

One question that remains is why levels of CIN that are elevated enough to suppress tumors do not adversely affect development, for instance in CENP-E $^{+/-}$; $Mad2^{+/-}$ doubly heterozygous mice. It is likely to be relevant that substantial cell death is required during normal embryonic development. In mammalian embryos, cell death begins early, between the 16-cell and blastula stages (39), and large numbers of cells are involved. Twenty to eighty percent of neurons, 80% of oocytes, and 95% of developing B cells are eliminated. In addition to these examples of the regulation of cell number, embryonic cells, such as those that constitute interdigital webs, are removed during organogenesis and tissue remodeling. Faulty and potentially dangerous cells, including immune cells that recognize self-antigens, virally infected cells, and those that contain unrepaired DNA damage, also undergo cell death during normal development (40, 41). Perhaps the effects of cell death resulting from high CIN are inconsequential in the context of this substantial level of programmed cell death.

Our data suggest that tumor suppression as a consequence of high CIN may depend on one or more cell-death pathways remaining intact. Consistent with this notion, reduction of the mitotic checkpoint components Bub1, Mad1, or Mad2 causes low CIN and an increased incidence of spontaneous tumors (25, 42, 43). However, combining low CIN resulting from the reduction of these components with low CIN resulting from p53 deficiency promotes tumors rather than suppressing them (44, 45). These results suggest that p53 may participate in eliminating cells exhibiting high CIN, although the specific functions of these proteins complicate this interpretation. Bub1, for instance, has been shown to mediate cell death in response to chromosome missegregation (42). Interestingly, reducing levels of Mad1 in animals doubly heterozygous for p53 and Mad2 actually suppresses the formation of lymphomas (46). Additional experiments will be required to determine the cell-death pathway(s) invoked by high CIN and the extent to which other death pathways can compensate.

The finding that increasing the rate of CIN in aneuploid cells can inhibit tumor initiation and/or progression raises the possibility that increasing CIN is a potential therapeutic avenue for the treatment of CIN tumors. Indeed, evidence from cell-culture experiments indicates that low CIN induced by reduction of BubR1 or Mps1 cooperates with low CIN resulting from small concentrations of taxol to cause high CIN and decreased cell viability (38). One concern about treatments that induce CIN is the potential for the generation of new tumors driven by CIN. However, CENP-E heterozygous animals are surprisingly normal given the high percentage of aneuploid cells they contain. Tumors that do form in these animals require a long latency to develop (19–21 mo), form within a narrow range of tissues, and occur with limited penetrance (10%). Multiple other mouse models that develop low CIN (Bub1^{+/-}, Bub1 kinase deficient, BubR1^{+/-}, Bub3^{+/-}, Rae1^{+/-}, Bub3^{+/-};Rae1^{+/-}, Cdc20^{+/-}, and animals hypomorphic for Separase) have long life expectancies and show no increase in spontaneous tumor development (37, 42, 47–52). It is now of interest to determine whether exacerbating chromosome missegregation in already chromosomally unstable tumors could serve as a useful therapeutic strategy. Indeed, enhanced chromosome missegregation may be one of the mechanisms, along with cell death from chronic arrest, through which low-dose taxol exerts its effects against tumors in vivo. Similarly, the CENP-E inhibitor tested in clinical trials (GSK923295) may be most useful in CIN tumors, including those of the lung, breast, and colon (53).

Materials and Methods

Cell Culture and Mouse Colony. Primary MEFs were generated from day E14.5 embryos as described (http://escorim.wustl.edu/SubMenu_protocols/protocol4.html). Primary MEFs were grown in DMEM supplemented with 15% (vol/vol) FBS, 0.1 mM nonessential amino acids (Gibco), 1 μM 2-mercaptoethanol (Specialty Media), 1 mM sodium pyruvate (Gibco), 2 mM glutamine, and 50 μg/mL penicillin/streptomycin in a 37 °C humidified incubator with 10% CO₂

and 3% oxygen. Low-oxygen conditions were used to extend the cycling time of the primary cells (54). DMBA was used at 50 μg/mL unless otherwise specified. Chromosome spreads and FISH were performed as reported in ref. 13. All mice were maintained in a C57BL/6 background and handled in accordance with the guidelines of the Institutional Animal Care and Use Committee of the University of California at San Diego. The 19- to 21-mo-old animals were anesthetized with isoflurane and killed by cervical dislocation. Tumors were fixed in 10% formalin overnight at room temperature and stored at 4 °C before being embedded in paraffin. Sections (5 μm thick) for FISH and for H&E staining were prepared by the University of California at San Diego histology core and were analyzed by Nissi Varki (Department of Pathology, University of California at San Diego School of Medicine, La Jolla, CA). Comparison of wild-type and CENP-E^{+/-} animals was reported previously (13).

Liver Analysis. Adenovirus particles (1.5 × 10⁹) carrying a gene encoding Cre recombinase or β-galactosidase were introduced into 2- to 3-mo-old male mice by tail vein injection, as described in ref. 11. Five to eleven days after injection, liver damage was induced by i.p. injection of 10 μL/g body weight of 20% carbon tetrachloride in olive oil. Livers were fixed in 10% formalin for at least 4 h at 4 °C, dehydrated in a graded series of ethanol, and embedded in paraffin wax. Archival sections stained with H&E were analyzed for the number of chromosomes missegregated per cell.

Immunofluorescence. Cells were washed with 37 °C microtubule-stabilizing buffer (MTSB) [100 mM Pipes, 1 mM EGTA, 1 mM MgSO₄, and 30% (wt/vol) glycerol] and were preextracted with 0.5% Triton X-100 in MTSB. After extraction, cells were washed again with MTSB and fixed in 4% formaldehyde (Tousimis Research Corporation) for 10 min. Triton Block [0.1% Triton X-100, 2.5% (vol/vol) FBS, and 200 mM glycine in PBS] was used to block cells and dilute antibodies. The DM1α antibody to α-tubulin (55) was diluted 1:1,000, Y11/2 rat monoclonal anti-α-tubulin (Serotec) was diluted 1:1,000, and anti-activated caspase 3 (Cell Signaling Technology) was diluted 1:100. Images were collected using a Nikon Ti-E or a DeltaVision wide-field deconvolution microscope system with a Nikon TE200 base. Chromosome spread images are from a single z-plane. For other images, optical sections were taken at 0.2-μm intervals and deconvolved using DeltaVision SoftWoRx software. Figures were generated using maximum projections.

Time-Lapse Microscopy. Chromosome segregation was observed in cells stably expressing histone H2B-RFP and grown in 35-mm dishes with glass bottoms in CO₂-independent medium (Invitrogen) supplemented with 10% (vol/vol) FBS, 2 mM L-glutamine, and 50 μg/mL penicillin/streptomycin and overlaid with sterile mineral oil. Five z-planes were acquired every 2 min using a 60× oil immersion objective and Metamorph software on a Nikon TE200 microscope. Maximum projections of in-focus planes were assembled in Metamorph and converted to .mov files in Quicktime.

ACKNOWLEDGMENTS. We thank Dr. Nissi Varki and the University of California at San Diego histology core for preparation and analysis of histological specimens and Melissa McAlonis-Downes for assistance with the mouse colony. This work was supported in part by National Institutes of Health (NIH) Grants R01-CA140458 (to B.A.W.) and R01-GM29513 (to D.W.C.) and by American Cancer Society Grant IRG-58-011-48 (to B.A.W.). L.M.Z. was supported in part by NIH Grant T32 GM008688. A.J.H. was supported by a Leukemia and Lymphoma Society senior fellowship. B.V. was supported by a postdoctoral fellowship from the Human Frontiers Cancer Program. D.W.C. receives salary support from the Ludwig Institute for Cancer Research.

1. von Hansemann D (1890) Ueber asymmetrische Zelltheilung in Epithelkrebsen und deren biologische Bedeutung. *Virchow's Arch. Path. Anat.* 119:299–326.
2. Boveri T (1902) Ueber mehrpolige Mitosen als Mittel zur Analyse des Zellkerns [On multipolar mitosis as a means of analysis of the cell nucleus]. *Vehr. d. phys. med. Ges. zu Wurzburg, N.F.* German. Available at <http://be.devbio.com/article.php?ch=4&id=24>.
3. Boveri T (1914) *The Origin of Malignant Tumors*; trans Boveri M (1929). (Williams and Wilkins, Baltimore).
4. Kops GJ, Foltz DR, Cleveland DW (2004) Lethality to human cancer cells through massive chromosome loss by inhibition of the mitotic checkpoint. *Proc Natl Acad Sci USA* 101(23):8699–8704.
5. Michel L, et al. (2004) Complete loss of the tumor suppressor MAD2 causes premature cyclin B degradation and mitotic failure in human somatic cells. *Proc Natl Acad Sci USA* 101(13):4459–4464.
6. Ganem NJ, Godinho SA, Pellman D (2009) A mechanism linking extra centrosomes to chromosomal instability. *Nature* 460(7252):278–282.
7. Kim Y, Heuser JE, Waterman CM, Cleveland DW (2008) CENP-E combines a slow, processive motor and a flexible coiled coil to produce an essential motile kinetochore tether. *J Cell Biol* 181(3):411–419.
8. Wood KW, Sakowicz R, Goldstein LS, Cleveland DW (1997) CENP-E is a plus end-directed kinetochore motor required for metaphase chromosome alignment. *Cell* 91(3):357–366.
9. Brown KD, Coulson RM, Yen TJ, Cleveland DW (1994) Cyclin-like accumulation and loss of the putative kinetochore motor CENP-E results from coupling continuous synthesis with specific degradation at the end of mitosis. *J Cell Biol* 125(6):1303–1312.
10. McEwen BF, et al. (2001) CENP-E is essential for reliable bioriented spindle attachment, but chromosome alignment can be achieved via redundant mechanisms in mammalian cells. *Mol Biol Cell* 12(9):2776–2789.
11. Putkey FR, et al. (2002) Unstable kinetochore-microtubule capture and chromosomal instability following deletion of CENP-E. *Dev Cell* 3(3):351–365.
12. Gudimchuk N, et al. (2013) Kinetochore kinesin CENP-E facilitates end-on microtubule attachment. *Nat Cell Biol* 15(9):1079–1088.
13. Weaver BA, Silk AD, Montagna C, Verdier-Pinard P, Cleveland DW (2007) Aneuploidy acts both oncogenically and as a tumor suppressor. *Cancer Cell* 11(1):25–36.
14. Abrieu A, Kahana JA, Wood KW, Cleveland DW (2000) CENP-E as an essential component of the mitotic checkpoint in vitro. *Cell* 102(6):817–826.

15. Weaver BA, et al. (2003) Centromere-associated protein-E is essential for the mammalian mitotic checkpoint to prevent aneuploidy due to single chromosome loss. *J Cell Biol* 162(4):551–563.
16. Rieder CL, Schultz A, Cole R, Sluder G (1994) Anaphase onset in vertebrate somatic cells is controlled by a checkpoint that monitors sister kinetochore attachment to the spindle. *J Cell Biol* 127(5):1301–1310.
17. Rieder CL, Cole RW, Khodjakov A, Sluder G (1995) The checkpoint delaying anaphase in response to chromosome monoorientation is mediated by an inhibitory signal produced by unattached kinetochores. *J Cell Biol* 130(4):941–948.
18. Fu Z, et al. (2009) Deficiencies in Chfr and Mlh1 synergistically enhance tumor susceptibility in mice. *J Clin Invest* 119(9):2714–2724.
19. Shoemaker AR, et al. (2000) Mlh1 deficiency enhances several phenotypes of Apc (Min)+ mice. *Oncogene* 19(23):2774–2779.
20. de Wind N, Dekker M, van Rossum A, van der Valk M, te Riele H (1998) Mouse models for hereditary nonpolyposis colorectal cancer. *Cancer Res* 58(2):248–255.
21. Duncan AW, et al. (2010) The ploidy conveyor of mature hepatocytes as a source of genetic variation. *Nature* 467(7316):707–710.
22. Duncan AW, et al. (2012) Frequent aneuploidy among normal human hepatocytes. *Gastroenterology* 142(1):25–28.
23. Han J-S, et al. (2013) Catalytic assembly of the mitotic checkpoint inhibitor BubR1-Cdc20 by a Mad2-induced functional switch in Cdc20. *Mol Cell* 51(1):92–104.
24. Dobles M, Liberal V, Scott ML, Benzra R, Sorger PK (2000) Chromosome mis-segregation and apoptosis in mice lacking the mitotic checkpoint protein Mad2. *Cell* 101(6):635–645.
25. Michel LS, et al. (2001) MAD2 haplo-insufficiency causes premature anaphase and chromosome instability in mammalian cells. *Nature* 409(6818):355–359.
26. Sherr CJ (2001) Parsing Ink4a/Arf: “Pure” p16-null mice. *Cell* 106(5):531–534.
27. Hernandez E, et al. (2004) Rb inactivation promotes genomic instability by uncoupling cell cycle progression from mitotic control. *Nature* 430(7001):797–802.
28. Lentini L, Pipitone L, Di Leonardo A (2002) Functional inactivation of pRB results in aneuploid mammalian cells after release from a mitotic block. *Neoplasia* 4(5):380–387.
29. Piboonyom SO, et al. (2003) Abrogation of the retinoblastoma tumor suppressor checkpoint during keratinocyte immortalization is not sufficient for induction of centrosome-mediated genomic instability. *Cancer Res* 63(2):476–483.
30. Baker DJ, et al. (2008) Opposing roles for p16Ink4a and p19Arf in senescence and ageing caused by BubR1 insufficiency. *Nat Cell Biol* 10(7):825–836.
31. Lengauer C, Kinzler KW, Vogelstein B (1997) Genetic instability in colorectal cancers. *Nature* 386(6625):623–627.
32. Søreide K, Janssen EA, Söiland H, Körner H, Baak JP (2006) Microsatellite instability in colorectal cancer. *Br J Surg* 93(4):395–406.
33. Rowland BD, Peeper DS (2006) KLF4, p21 and context-dependent opposing forces in cancer. *Nat Rev Cancer* 6(1):11–23.
34. Serrano M, Lin AW, McCurrach ME, Beach D, Lowe SW (1997) Oncogenic ras provokes premature cell senescence associated with accumulation of p53 and p16INK4a. *Cell* 88(5):593–602.
35. Evan GI, et al. (1992) Induction of apoptosis in fibroblasts by c-myc protein. *Cell* 69(1):119–128.
36. Bringold F, Serrano M (2000) Tumor suppressors and oncogenes in cellular senescence. *Exp Gerontol* 35(3):317–329.
37. Baker DJ, et al. (2004) BubR1 insufficiency causes early onset of aging-associated phenotypes and infertility in mice. *Nat Genet* 36(7):744–749.
38. Janssen A, Kops GJ, Medema RH (2009) Elevating the frequency of chromosome mis-segregation as a strategy to kill tumor cells. *Proc Natl Acad Sci USA* 106(45):19108–19113.
39. Hardy K, Handyside AH, Winston RM (1989) The human blastocyst: Cell number, death and allocation during late preimplantation development in vitro. *Development* 107(3):597–604.
40. Fuchs Y, Steller H (2011) Programmed cell death in animal development and disease. *Cell* 147(4):742–758.
41. Penalzo C, Lin L, Lockshin RA, Zakeri Z (2006) Cell death in development: Shaping the embryo. *Histochem Cell Biol* 126(2):149–158.
42. Jeganathan K, Malureanu L, Baker DJ, Abraham SC, van Deursen JM (2007) Bub1 mediates cell death in response to chromosome missegregation and acts to suppress spontaneous tumorigenesis. *J Cell Biol* 179(2):255–267.
43. Iwanaga Y, et al. (2007) Heterozygous deletion of mitotic arrest-deficient protein 1 (MAD1) increases the incidence of tumors in mice. *Cancer Res* 67(1):160–166.
44. Baker DJ, Jin F, Jeganathan KB, van Deursen JM (2009) Whole chromosome instability caused by Bub1 insufficiency drives tumorigenesis through tumor suppressor gene loss of heterozygosity. *Cancer Cell* 16(6):475–486.
45. Li M, et al. (2010) The ATM-p53 pathway suppresses aneuploidy-induced tumorigenesis. *Proc Natl Acad Sci USA* 107(32):14188–14193.
46. Chi YH, Ward JM, Cheng LI, Yasunaga J, Jeang KT (2009) Spindle assembly checkpoint and p53 deficiencies cooperate for tumorigenesis in mice. *Int J Cancer* 124(6):1483–1489.
47. Ricke RM, van Ree JH, van Deursen JM (2008) Whole chromosome instability and cancer: A complex relationship. *Trends Genet* 24(9):457–466.
48. Holland AJ, Cleveland DW (2009) Boveri revisited: Chromosomal instability, aneuploidy and tumorigenesis. *Nat Rev Mol Cell Biol* 10(7):478–487.
49. Ricke RM, Jeganathan KB, Malureanu L, Harrison AM, van Deursen JM (2012) Bub1 kinase activity drives error correction and mitotic checkpoint control but not tumor suppression. *J Cell Biol* 199(6):931–949.
50. Malureanu L, et al. (2010) Cdc20 hypomorphic mice fail to counteract de novo synthesis of cyclin B1 in mitosis. *J Cell Biol* 191(2):313–329.
51. Baker DJ, et al. (2006) Early aging-associated phenotypes in Bub3/Rae1 haploinsufficient mice. *J Cell Biol* 172(4):529–540.
52. Mukherjee M, et al. (2011) Separase loss of function cooperates with the loss of p53 in the initiation and progression of T- and B-cell lymphoma, leukemia and aneuploidy in mice. *PLoS ONE* 6(7):e22167.
53. Wood KW, et al. (2010) Antitumor activity of an allosteric inhibitor of centromere-associated protein-E. *Proc Natl Acad Sci USA* 107(13):5839–5844.
54. Parrinello S, et al. (2003) Oxygen sensitivity severely limits the replicative lifespan of murine fibroblasts. *Nat Cell Biol* 5(8):741–747.
55. Blose SH, Meltzer DI, Feramisco JR (1984) 10-nm filaments are induced to collapse in living cells microinjected with monoclonal and polyclonal antibodies against tubulin. *J Cell Biol* 98(3):847–858.

Supporting Information

Silk et al. 10.1073/pnas.1317042110

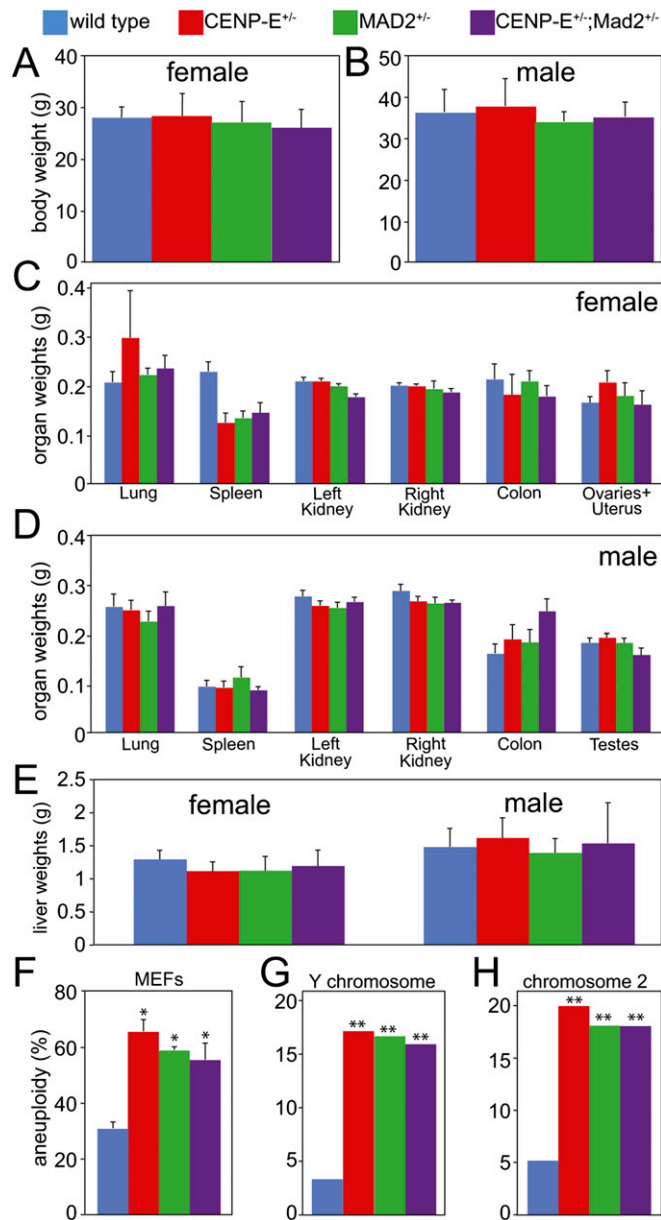


Fig. S1. Mice with elevated levels of aneuploidy have normal organ and body weights. (A and B) Average weights of 19- to 21-mo-old female (A) and male (B) mice of the indicated genotypes. (C and D) Average weights of the indicated organs in female (C) and male (D) mice. (E) Average weights of livers in female (Left) and male (Right) mice of the indicated genotypes. (F) Average aneuploidy in chromosome spreads of primary murine embryonic fibroblasts (MEFs) at passage 3 and 4. ($n = 50$ spreads from each of three independent experiments; $*P < 0.05$ compared with wild-type). (G and H) Aneuploidy in large intestine as assessed by interphase FISH using probes for the Y chromosome (G) or chromosome 2 (H). ($n \geq 250$ cells; $**P < 0.001$ compared with wild-type).

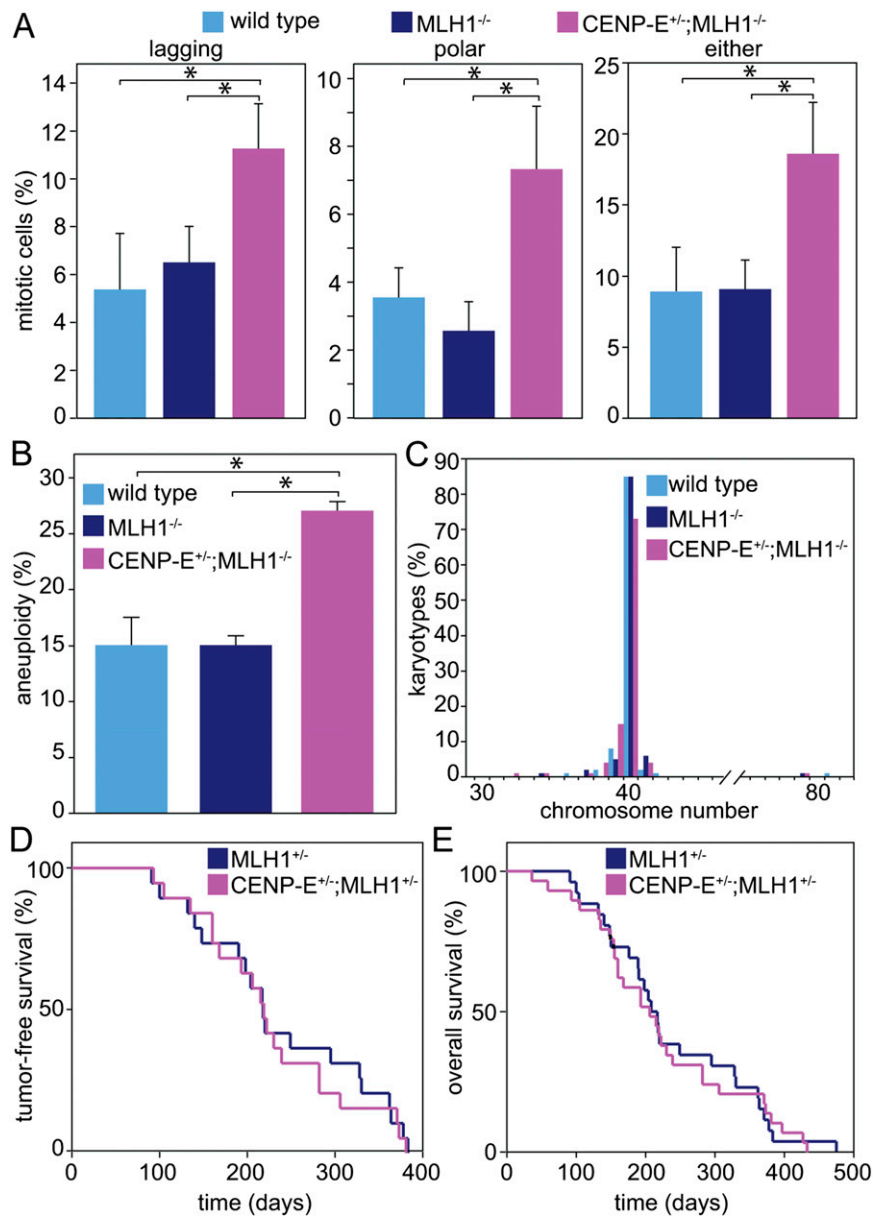
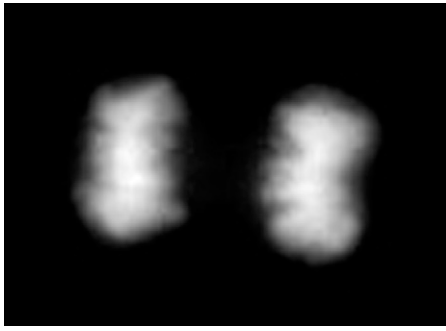
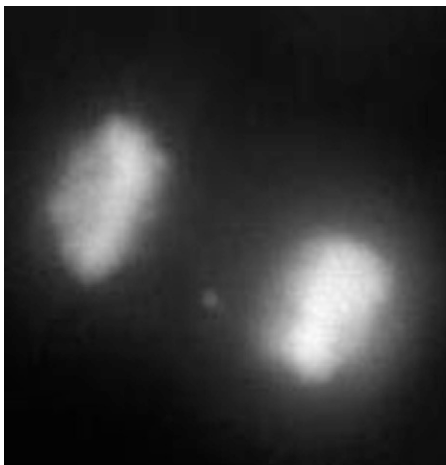


Fig. S3. Chromosomal instability and microsatellite instability do not produce combinatorial effects on tumor onset. (A–C) Measurement of aneuploidy and chromosomal instability in varying cell genotypes. Loss of MLH1 does not cause chromosome missegregation or aneuploidy. (A) Lagging or polar chromosomes measured in MLH1^{-/-} MEFs with normal or reduced CENP-E ($n \geq 150$ cells from each of three independent experiments). (B) Aneuploidy, as assessed by chromosome spreads, in wild-type or MLH1^{-/-} MEFs with normal or reduced CENP-E. (C) Histogram showing near diploid aneuploidy in CENP-E^{+/-};MLH1^{-/-} MEFs. (In B and C, $n = 100$ cells from two independent experiments.) (D) Tumor-free survival of MLH1^{+/-} animals with normal and reduced levels of CENP-E ($n = 19$ for both MLH1^{+/-} and CENP-E^{+/-};MLH1^{+/-} animals; log rank P value = 0.83). (E) Overall survival of 26 MLH1^{+/-} and 29 CENP-E^{+/-};MLH1^{+/-} animals (log rank P value = 0.87).



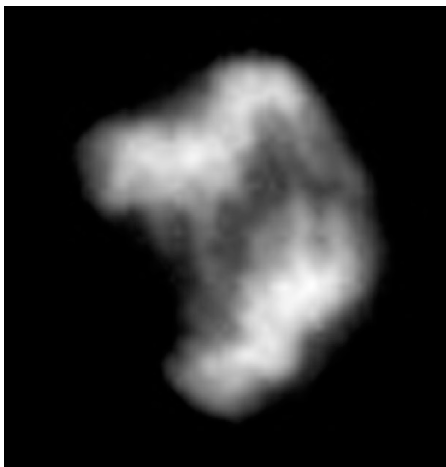
Movie S1. Time-lapse movie of normal mitosis in the primary MEF shown in Fig. 1J. DNA was visualized in cells stably expressing H2B-RFP. Five z-planes were acquired using a 60 \times objective every 2 min.

[Movie S1](#)



Movie S2. Time-lapse movie of the ARF^{-/-} MEF with a lagging chromosome presented in Fig. 1K. DNA was visualized in cells stably expressing H2B-RFP. Five z-planes were acquired using a 60 \times objective every 2 min.

[Movie S2](#)



Movie S3. Time-lapse movie of the CENP-E^{+/-};ARF^{-/-} primary MEF missegregating multiple chromosomes shown in Fig. 1L. DNA was visualized in cells stably expressing H2B-RFP. Five z-planes were acquired using a 60 \times objective every 2 min.

[Movie S3](#)